ACS Catalysis

Research Article

pubs.acs.org/acscatalysis

Pulse and IR Study on the Reaction Pathways for the Conversion of Ethanol to Propene over Scandium-Loaded Indium Oxide Catalysts

Masakazu Iwamoto,*[,†] Masashi Tanaka,[†] Shota Hirakawa,[‡] Shota Mizuno,[‡] and Mika Kurosawa[‡]

[†]Research and Development Initiative, Chuo University, 1-13-27 Kasuga, Bunkyo-ku, Tokyo 112-8551, Japan

[‡]Chemical Resources Laboratory, Tokyo Institute of Technology, 4259 Nagatsuta, Midori-ku, Yokohama 226-8503, Japan

Supporting Information

ABSTRACT: Potential reaction intermediates in the conversion of ethanol to propene, acetaldehyde, ethyl acetate, crotonaldehyde, acetic acid, acetone, and 2-propanol were introduced as pulses onto a scandium-loaded indium oxide catalyst. The product distributions were primarily measured as a function of the space velocity in the absence or presence of hydrogen and water. The FT-IR spectra of the surface adsorbates were also collected after ethanol adsorption and indicated the formation of ethoxide species, which were converted to acetate species over the catalyst. The proposed reaction route involved the dehydrogenation of ethanol to acetaldehyde, direct oxidation of acetaldehyde with water or a surface hydroxyl group to yield acetic acid, ketonization of acetic acid to acetone and carbon dioxide, and hydrogenation and subsequent dehydration of acetone to propene. The total reaction can be described as 2 $CH_3CH_2OH \rightarrow CH_2{=}CHCH_3 + CO_2 + 3\ H_2$. A side reaction involving isobutene formation also occurred via the acetone intermediate.

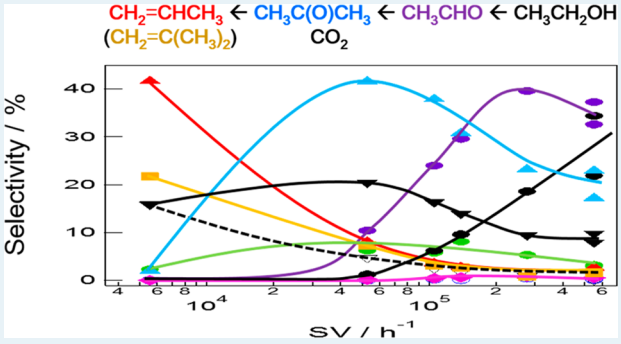

KEYWORDS: *ethanol, propene, indium oxide, scandium, acetate, ketonization*

INTRODUCTION

The catalytic conversion of ethanol to propene[1−12] has very recently been developed to use bioethanol as a starting material for chemicals and reduce the carbon dioxide emission from naphtha crackers. Among the active catalysts that have been developed, Ni ion-loaded mesoporous silica MCM-41 (Ni-M41),[8−10] yttrium loaded cerium oxides (Y/CeO_2),[11] and scandium-modified indium oxides (Sc/In_2O_3),[12] Sc/In_2O_3 results in good propene yields and long durability. Therefore, the elucidation of the reaction pathways on the catalyst would be useful for understanding the catalytic process and improving the activity.

The possible reaction pathways on the oxide catalysts for the conversion of ethanol to propene are summarized in Figure 1, where the notations of the compounds indicate that they might be generated as intermediate products or surface intermediates. The reaction pathways over zeolite catalysts[3−5] were not included in this figure. Oligomerization, aromatization, and fission reactions on strong acid sites in zeolite pores are widely known to result in the formation of ethene, propene, and butenes due to shape selectivity. However, these uncontrolled reactions that occur in the pores ultimately result in coke formation and short catalyst life times. Therefore, the reaction pathways over zeolites have been omitted here. There are two ethanol reaction routes including dehydration to yield ethene (Pathway 1) and dehydrogenation to afford acetaldehyde (Pathway 6), that can occur over oxide catalysts.[6−12] Our

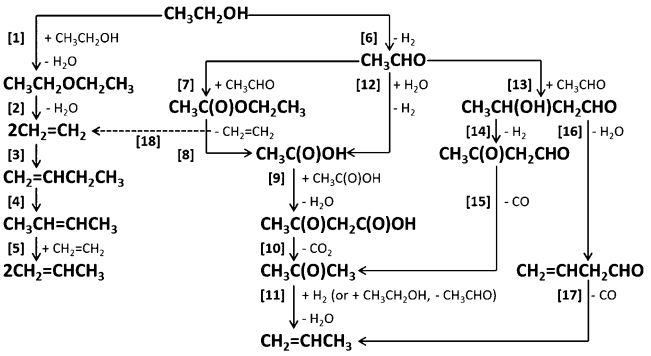

Figure 1. Proposed reaction pathways for the conversion of ethanol to propene over oxide catalysts.

recent paper on Ni-M41[9] revealed that ethene produced through Pathways 1 and 2 or Pathways 6, 7, 8, and 18 was an intermediate in the production of propene. Ethene was dimerized to form 1-butene, which was isomerized to 2-butenes. The resulting 2-butenes could react with another ethene to produce propene via metathesis. The progress of the metathesis reaction on Ni-M41 was confirmed in separate

Received: July 15, 2014
Revised: August 24, 2014
Published: August 25, 2014

   dx.doi.org/10.1021/cs5006822 | ACS Catal. 2014, 4, 3463−3469

experiments.[13] The acetic acid that is coproduced through Pathways 6, 7, and 8 would react with ethanol or hydrogen to form ethyl acetate (eq 1), acetaldehyde (eq 2), or ethanol (eq 3), as reported over several catalysts.[6,7] Equation 1 is well-known as the Fisher esterification. These equations suggested the circulation of acetic acid on the Ni-M41 catalyst.

$$CH_3COOH + CH_3CH_2OH \rightarrow CH_3COOCH_2CH_3 + H_2O \quad (1)$$

$$CH_3COOH + H_2 \rightarrow CH_3CHO + H_2O \quad (2)$$

$$CH_3COOH + 2H_2 \rightarrow CH_3CH_2OH + H_2O \quad (3)$$

On the Y/CeO_2 catalyst, the simultaneous production of ethene and propene was observed in the presence/absence of water. The reactivity of ethyl acetate was studied using pulse experiments, which indicated its decomposition through Pathway 8.[11] The produced ethene was observed without any further reactions. However, acetic acid was converted to acetone through ketonization (Pathways 9 and 10). Acetone was converted to propene by cofed ethanol (Pathway 11), which involved the reduction of acetone by ethanol (eq 4) and the subsequent dehydration of 2-propanol to propene (eq 6). Equation 4 is known as the Meerwein−Ponndorf−Verley (MPV) reduction.[14]

$$CH_3C(O)CH_3 + CH_3CH_2OH \rightarrow CH_3CH(OH)CH_3 + CH_3CHO \quad (4)$$

$$CH_3C(O)CH_3 + H_2 \rightarrow CH_3CH(OH)CH_3 \quad (5)$$

$$CH_3CH(OH)CH_3 \rightarrow CH_2 = CHCH_3 + H_2O \quad (6)$$

The reaction pathways 1−11 in Figure 1, in which Pathway 11 on Y/CeO_2 was the MPV reduction, were already suggested on Ni-M41 or Y/CeO_2. In contrast to the reactions on these catalysts, the amount of ethene produced on the Sc/In_2O_3 catalysts was very small, and isobutene was one of the major products.[12] In addition, the production ratios of acetone/propene/isobutene, as well as the durability of the catalyst, were dependent on the partial pressures of water and hydrogen. These findings indicated that the reaction pathways on Sc/In_2O_3 are different from those over Ni-M41 and Y/CeO_2 and should be studied separately.

Initially, we measured the contact time dependence of the product distribution in a continuous flow system but did not obtain significant conclusions due to complicated product distributions. Therefore, a pulse technique was applied to determine the reactivity of several potential intermediate compounds and determine the reaction pathways. As summarized in the Experimental Section, we constructed a new apparatus for the pulse experiments in which various substrates could be introduced into the carrier gas flows containing water or hydrogen because the presence of water and hydrogen in the reactant flows was previously reported to substantially improve the propene yield and catalyst durability.[12] In addition, surface adsorbates on the Sc/In_2O_3 catalyst were investigated using FT-IR measurements to confirm the reaction pathways.

EXPERIMENTAL SECTION

Materials. Indium oxide, In_2O_3 (4.2 m^2g^{-1}, BET surface area after calcination at 1073 K for 5 h), was commercially obtained from the Kanto Chemical Co. Japan. Scandium-loaded In_2O_3 samples were prepared by a conventional impregnation method using acetate salt. The detailed preparation method is described in a previous paper.[12] The scandium loading was 3 atomic % to that of In, whose amount was determined by an induced coupled plasma analysis after the samples were dissolved in HF solutions. The catalysts were calcined at 1073 K for 5 h, and the respective grain sizes were adjusted to 0.3−0.6 mm for use in catalytic runs. The catalyst was designated as $Sc3/In_2O_3$, where "3" was the atomic % of loaded scandium.

Ethanol and the other organic reagents were purchased commercially from the Kanto Chemical Co. Japan, and used without further purification.

Apparatus and General Procedure for the Pulse Experiments. As reported in the previous paper,[12] the coexistence of water or hydrogen in the continuous flow experiments substantially improved the selectivity to propene and the durability of the Sc/In_2O_3 catalysts. The cointroduction of water or hydrogen with ethanol or other substrates as one pulse is one method for determining the addition effect. For example, in these experiments, the mixture of acetaldehyde and water is introduced onto the catalyst dried upon heating in the carrier gas flow. Therefore, it is possible that the product distribution is different from that on a wet catalyst surface in typical continuous flow systems. Similarly, the presence or absence of hydrogen atoms preadsorbed on the catalyst might greatly influence the dehydrogenation and hydrogenation reactions. On the basis of these considerations, we employed mixed flows of H_2O/N_2 or H_2/N_2 as the carrier gas in the pulse experiments. However, the carrier gas in the reactor was also employed as the carrier in the gas chromatograph system in the typical pulse experiment apparatus. Therefore, this mixture cannot be employed as the carrier gas. The carrier gas for the gas chromatography system was segregated from the carrier gas for the catalytic reaction in the current experimental apparatus for the pulse experiments. A thermal conductivity detector (TCD) was installed after the catalyst bed, and a sampling loop consisting of a six-way valve was also attached after the TCD. In the pulse experiments, the flow of products after substrate injection was detected by the TCD, and the sampling loop automatically picked up the portion of products according to the TCD signal and sent it to the gas chromatography system.

Pulse experiments using various substrates were performed in a quartz microreactor with an inner diameter of 7.6 mm at atmospheric pressure. Prior to each reaction, 0.1−2.0 g of the catalyst mounted in the reactor was treated at 673 K in N_2 (50 mL/min) for 60 min to remove any residual gases in the system followed by exposure to the pulses (a 2 μL aliquot of a liquid sample). The products were analyzed with an online automatic gas chromatograph (GC7100, J-Science, Japan) equipped with four packed columns and a capillary column as follows: activated charcoal, MS 5A, Porapak Q, and PEG-20M, and GS-Q (30 m, Agilent, U.S.A.). The change in the catalytic activity with the reaction time (durability) was analyzed by the occasional injection of ethanol and the consistency of the product distributions within the experimental errors. The conversion and selectivity were calculated on the basis of the carbon content in the products assuming a 100% carbon balance.

IR Measurements of Surface Adsorbates. The FT-IR spectra were recorded at room temperature using a JASCO FTIR-6300 spectrophotometer with a MCT detector (accumulation 32 scans, resolution 4 cm^{-1}). The powdered sample was pressed into a self-supporting disk with a diameter of 10 mm and placed in a quartz cell with KRS-5 windows. The cell was capable of in situ treatment and gas introduction. The

dx.doi.org/10.1021/cs5006822 | ACS Catal. 2014, 4, 3463−3469

adsorption measurement of ethanol or acetic acid was performed by introducing the gas at room temperature to the $Sc3/In_2O_3$ sample pre-evacuated at 673 K.

RESULTS AND DISCUSSION

Confirmation of Overall Reaction Yielding Propene. The conversion of ethanol to propene on $Sc3/In_2O_3$ has been proposed to proceed via an acetone intermediate. The overall reactions for the formation of propene can be described as shown in eq 7. The acetone formation is described by eq 8.[12,15,16]

$$2CH_3CH_2OH \rightarrow CH_2{=}CHCH_3 + CO_2 + 3H_2 \quad (7)$$

$$2CH_3CH_2OH + H_2O \rightarrow CH_3C(O)CH_3 + CO_2 + 4H_2 \quad (8)$$

$$3CH_3CH_2OH + H_2O \rightarrow CH_2{=}C(CH_3)_2 + 2CO_2 + 6H_2 \quad (9)$$

$$CO_2 + H_2 \rightarrow CO + H_2O \quad (10)$$

$$A_{C3}/3 + A_{C4}/2 = A_{CO_x} \quad (11)$$

The molar ratio of the total amounts of propene and acetone, A_{C3}, with those of carbon dioxide, A_{CO_2}, were 3:1 based on eqs 7 and 8. In the calculation, the A_{CO_2} values should be replaced with the total amounts of carbon dioxide and carbon monoxide, A_{CO_x}, because the progress of eq 10 was confirmed on the catalyst. In addition, because the isobutene formation was accompanied by CO_2 formation (eq 9), the A_{C3} values should be corrected for the quantities of isobutene, A_{C4}. eq 11 needs to be confirmed.

The product distributions in the flow system were employed to confirm the validity of the above equations. Typical results are shown in Figure 2 where the catalysis was investigated

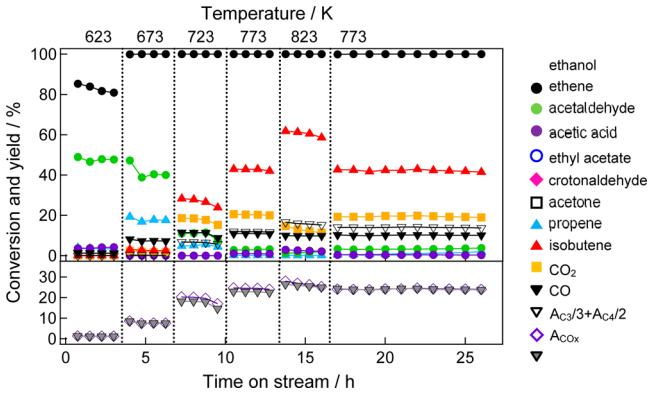

Figure 2. Catalytic activity of $Sc3/In_2O_3$ (the upper row) and a comparison of $A_{C3}/3 + A_{C4}/2$ with A_{CO_x} (the lower) as a function of the reaction time and temperature. Reaction conditions: catalyst weight, 2.0 g; total flow rate, 12.8 mL min^{-1} (GHSV 687 h^{-1}); 1 atm; P_{EtOH}, 30 vol %; P_{H_2O}, 8.5 vol %; P_{H_2}, 30 vol %; N_2 balance.

under various reaction temperatures and times over $Sc3/In_2O_3$.[12] The upper column of the figure shows the amounts of ethanol reacted and the distributions of hydrocarbons produced, whereas the lower one summarizes the amounts of CO_2 + CO and the values of $A_{C3}/3 + A_{C4}/2$. Equation 11 was confirmed by the results in the lower column irrespective of the experimental conditions, which supports the occurrence of the total reactions shown in eqs 7−9.

Reaction Pathways of Ethanol and Acetaldehyde. The product distributions in the pulse experiments of ethanol were determined at 773 K as a function of the gas hourly space velocity (GHSV) and are summarized in Figure 3a. Unreacted

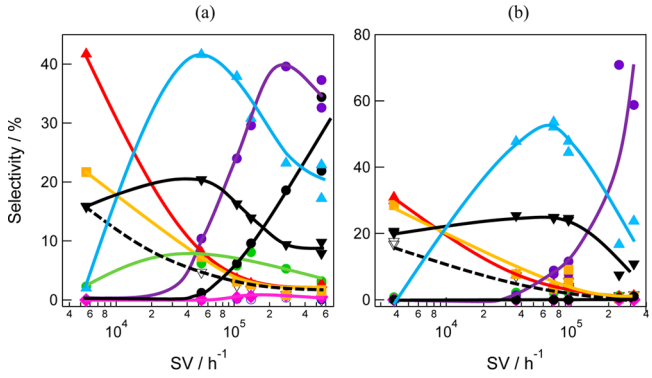

Figure 3. Product distributions upon introduction of ethanol (a) and acetaldehyde (b) pulses at 773 K in a N_2 flow. The distributions were measured as a function of GHSV. The symbols are the same as those shown in Figure 1.

ethanol was detected at 500 000 h^{-1} but it disappeared at approximately 80 000 h^{-1}. The first observed product was acetaldehyde whose amount was maximized at 300 000 h^{-1} and decreased at lower SVs. Acetone became the main product at 50 000 h^{-1}, which was accompanied by the coproduction of CO_2. At 5000 h^{-1}, the amounts of acetone and CO_2 decreased and those of propene, isobutene, and CO increased. The reactivity of acetaldehyde was studied separately and is summarized in Figure 3b. The change in the product distributions with SV was similar to that of ethanol even though the amount of propene produced was smaller than that in the reaction of ethanol (Figure 3a) due to the smaller amount of hydrogen, as mentioned below. These results indicated that acetaldehyde was the true intermediate in the conversion of ethanol to propene. All of the results clearly indicated the reaction sequence of ethanol → acetaldehyde → acetone (and CO_2) → propene and isobutene, which supports the proposed schemes shown in Figure 1.

Next, the reaction sequences for the formation of C_{2x-1} ketones from C_x-aldehydes on the Sc/In_2O_3 were investigated. Three types of pathways have been proposed for the oxide-based catalysts including the (i) aldol reaction,[15] (ii) Tishchenko reaction,[15] and (iii) ketonization reaction of carboxylic acids,[17] as shown in Figure 1. The aldol reaction of acetaldehyde yields 3-hydroxybutylaldehyde, which can be converted to $CH_3C(O)CH_2CHO$ or $CH_3CH{=}CHCHO$ by dehydrogenation (Pathway 14) or dehydration (16). Although the latter cannot produce acetone, the reactivity was studied. As shown in Figure 4a, crotonaldehyde was easily converted to propene with the release of CO (and CO_2), but no acetone was produced. The results indicated that crotonaldehyde was not involved in the reaction pathways over the Sc/In_2O_3. *β*-Ketoaldehyde has the potential to yield acetone through the release of CO (Pathway 15) or by reaction with water (yielding acetone, CO_2, and H_2). Because unstable *β*-hydroxyaldehyde and *β*-ketoaldehyde cannot be used as substrates in the current experiments, the products produced in Figure 2 were carefully analyzed using an off-line capillary GC system. However, no production of these compounds was observed, which suggested that the aldol reaction route was unlikely. The formation of ethyl acetate, acetic acid, and 2-propanol was confirmed in the current experiments. Therefore, the possibilities of the ethyl

dx.doi.org/10.1021/cs5006822 | ACS Catal. 2014, 4, 3463−3469

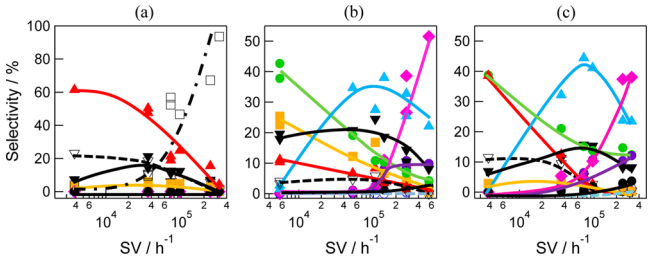

Figure 4. Product distributions upon introduction of crotonaldehyde (a) and ethyl acetate (b, c) pulses at 773 K in a N_2 (a, b) or H_2 (c) flow. The distributions were measured as a function of GHSV. The symbols are the same as those shown in Figure 1.

acetate route[15,16] and the direct path forming acetic acid[17] were investigated.

Figure 4b,c show the results from the pulse experiments of ethyl acetate as a function of the space velocity. In the absence of hydrogen (Figure 4b), the major product was acetone at high SVs and ethene at low SVs, and the yields of propene were lower than those in the flow system. In the presence of hydrogen (Figure 4c), the product distributions (acetone, CO_2, and ethene) were essentially similar to those without hydrogen (Figure 4b), though the propene and isobutene selectivities were substantially changed with/without hydrogen and almost replaced each other. The selective formation of ethene indicated the progress of Pathway 8, which was very different from the product distributions in the flow system shown in Figure 2. Therefore, ethyl acetate was not an intermediate in propene formation on the Sc/In_2O_3 catalysts. The small amount of ethyl acetate that was observed in the flow system as described above is a byproduct from acetic acid and ethanol due to the Fisher esterification (eq 1).

Acetic Acid as an Intermediate. The introduction of acetic acid in the absence or presence of hydrogen resulted in the products shown in Figure 5a,b. The amount of unreacted

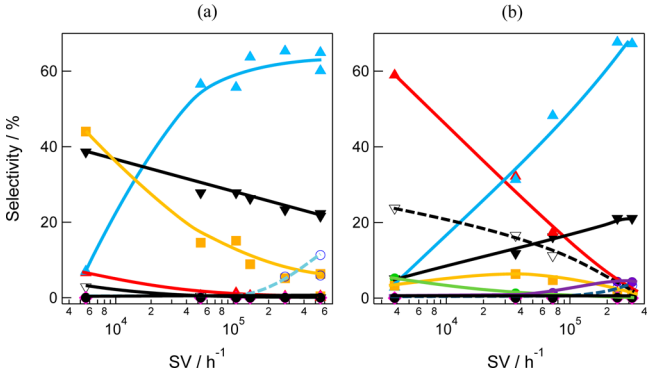

Figure 5. Product distributions upon introduction of acetic acid pulses at 773 K in a N_2 (a) or H_2 (b) flow. The distributions were measured as a function of GHSV. The symbols are the same as those shown in Figure 1.

acetic acid was very small even at high SVs, which indicated a very high reactivity of acetic acid over the catalyst. Acetic acid was selectively converted to acetone and CO_2 with a short contact time irrespective of the presence and absence of hydrogen. The ratio of acetone to CO_2 was approximately 3:1 (carbon basis) except for the ratio obtained at long contact times. The results confirmed the very easy and selective ketonization of acetic acid (Pathways 9 and 10). In addition, the resulting acetone was converted to propene and isobutene in the presence and absence of hydrogen, respectively, with increasing contact time. The reaction of acetone will be discussed in more detail below, and the acetic acid formation pathway will be discussed here.

Acetic acid is known to be generated from acetaldehyde under oxidative conditions, but this reaction was not observed here due to the absence of oxygen.[18] However, the direct reaction of an adsorbate (CH_3CH_2O) with a surface OH group has been proposed to generate the CH_3COO species on the oxide surface,[4,18] which might lead to the formation of acetic acid through one of several possible pathways such as Pathway 12. This possibility was examined using the pulse technique, and the results are summarized in Figure 6 as a function of

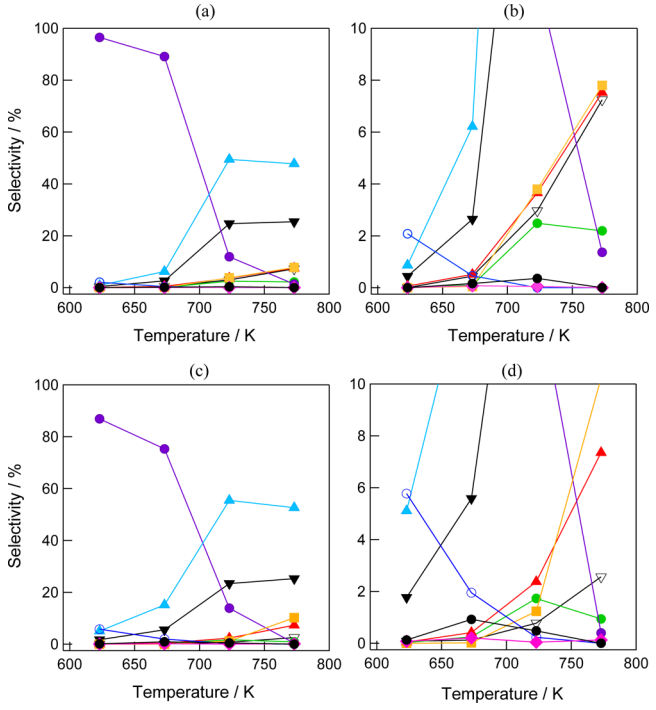

Figure 6. Product distributions upon introduction of acetaldehyde pulses at GHSV of 36,311 h^{-1} in a N_2 flow (a, b) or a mixed flow of N_2 and H_2O (P_{H_2O} = 10 vol %) (c, d). The distributions were measured as a function of reaction temperature. Panels (b) and (d) provide enlarged views of panels (a) and (c). The symbols are the same as those shown in Figure 1.

reaction temperature because the very high reactivity of acetic acid at 773 K might hide the appearance of acetic acid as an intermediate (product). A small amount of acetic acid was produced at 623 and 673 K in the absence of water, and its amount increased in the presence of water. In addition, the conversion levels of acetaldehyde also increased at these temperatures due to the addition of water to the reaction system. These observations indicated the true progress of the reaction of acetaldehyde with water to form acetic acid (Pathway 12), in which the water addition increased the reaction rate of acetaldehyde. The high reactivity of acetic acid would result in its minor appearance as the intermediary product in the experiments (Figures 2 and 3).

The surface intermediates were directly observed on the $Sc3/In_2O_3$ catalyst using FT-IR measurements. Typical results are shown in Figure 7 as a function of sample temperature. The

dx.doi.org/10.1021/cs5006822 | ACS Catal. 2014, 4, 3463−3469

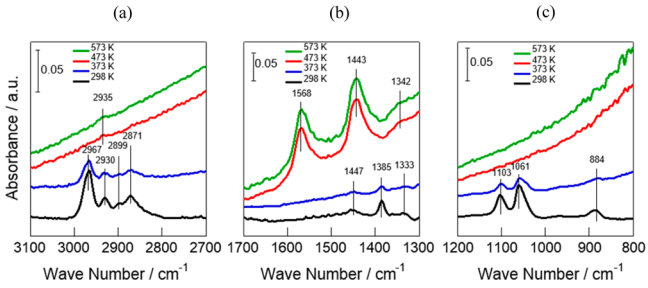

Figure 7. FT-IR spectra of the surface species adsorbed on the Sc3/In_2O_3 catalyst. Ethanol was adsorbed at room temperature on the self-standing wafer of the catalyst after the pretreatment mentioned in the text, and then, the sample temperature was gradually increased under a dynamic vacuum. The vibrations of the C−H, O−C−O, and C−O bonds are depicted in the panels (a), (b), and (c).

ethanol adsorption induced the appearance of surface ethoxide species[19,20] at 2967 cm^{-1} (assignable to $\nu_{as}(CH_3)$), 2930 ($\nu_{as}(CH_2)$), 2899 ($\nu_s(CH_3)$), 2871 ($\nu_s(CH_2)$), 1447 ($\delta_{as}(CH_3)$), and 1385 ($\delta_s(CH_3)$), 1104 ($\nu(CO)_{mono}$), 1061 ($\nu(CO)_{bi}$), and 884 ($\nu(CCO)$). This species was converted to acetate species[21−24] upon heating the sample to 473 K or higher, which was characterized by the absorptions at 2935 cm^{-1} ($\nu_s(CH_3)$), 1568 ($\nu_{as}(OCO)$), and 1443 ($\nu_s(OCO)$). The results indicated the surface reaction involved the conversion of ethanol to acetic acid, which is consistent with the results from the pulse experiments. All of the results in Figures 5−7 indicated that Pathway 12 was the primary route for the conversion of ethanol to acetic acid (then to acetone) on the Sc/In_2O_3 catalyst.

Conversion of Acetone to Propene. Finally, the conversion of acetone to propene was investigated. As reported previously, on the Y/CeO_2 catalyst, acetone was reduced to 2-propanol by unreacted ethanol (i.e., the MPV reduction) and not by gaseous hydrogen. The reaction of acetone on the current Sc/In_2O_3 catalyst was studied, and the results are summarized in Figure 8a,b. In the presence of hydrogen (Figure

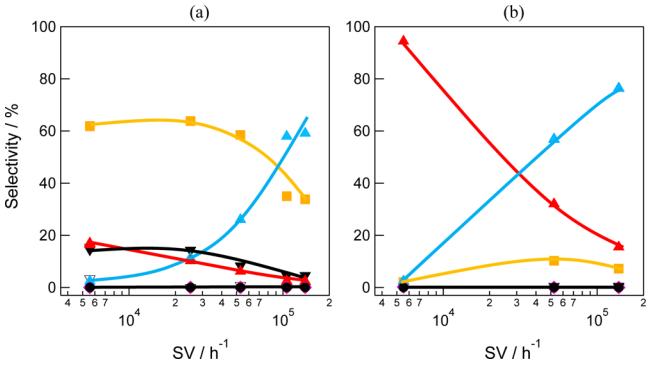

Figure 8. Product distributions upon introduction of acetone pulses at 773 K in a N_2 (a) or H_2 (b) flow. The distributions were measured as a function of GHSV. The symbols are the same as those shown in Figure 1.

8b), acetone was selectively converted to propene along with a small amount of isobutene byproduct. The maximum yield of propene reached 94% at low SV, which indicated that the reaction of acetone with hydrogen was facile, in contrast to the reaction on Y/CeO_2, and yielded propene. The production of 2-propanol was not significant, which was most likely due to very rapid conversion of 2-propanol to propene or the low desorption rate of the 2-propanol intermediate. In contrast, in the absence of hydrogen (Figure 8a), isobutene was the major product along with a small amount of propene byproduct. This result indicated the progress of the selective conversion of acetone to isobutene, which has been previously reported for the $Zn_xZr_yO_z$ catalyst.[16] Similar results were observed in Figure 5a,b where acetic acid was used as the substrate. The conversion of acetone to isobutene can be formally expressed by eq 12 even though the reaction mechanism is unknown and the acetic acid byproduct cannot be confirmed due to its very rapid conversion. The total reaction from ethanol to isobutene is expressed in eq 9.

$$2CH_3C(O)CH_3 \rightarrow CH_2 = C(CH_3)_2 + CH_3C(O)OH \quad (12)$$

The reactivity of 2-propanol is summarized in Figures 9a,b. Even at the highest space velocity studied, the remaining 2-

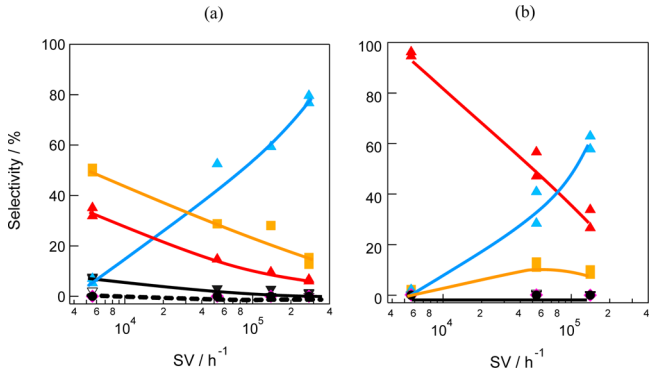

Figure 9. Product distributions upon introduction of 2-propanol pulses at 773 K in a N_2 (a) or H_2 (b) flow. The distributions were measured as a function of GHSV. The symbols are the same as those shown in Figure 1.

propanol was barely observed irrespective of the presence/absence of hydrogen, which indicated its very high reactivity. The characteristic product in both experiments was acetone. The major product was acetone at a high space velocity, and the amount decreased as the SV decreased. Therefore, the reverse reaction of eq 5 (eq 13), which has a large rate constant, occurred on Sc/In_2O_3. The produced acetone was hydrogenated to 2-propanol in the presence of hydrogen and then dehydrated to propene (Figure 9b) or converted to isobutene in the absence of hydrogen (Figure 9a). The results indicated that the reactions between acetone + hydrogen and 2-propanol were reversible and the equilibrium was biased to the acetone side.

$$CH_3CH(OH)CH_3 \rightarrow CH_3C(O)CH_3 + H_2 \quad (13)$$

On the basis of the above results and discussion, the following reaction pathways yielding propene from ethanol was proposed for the Sc-modified In_2O_3 catalyst. Ethanol was dehydrogenated to acetaldehyde, and the resulting acetaldehyde was converted to acetic acid via oxidation with water or surface hydroxyl groups. The acetic acid yielded acetone and carbon dioxide via the ketonization reaction. Propene was produced by the hydrogenation of acetone with hydrogen followed by dehydration. It would be worthy to discuss which reaction is the rate-determining step in the consecutive reactions on Sc/In_2O_3. As shown in Figure 3a, the observed intermediates in the pulse experiments of ethanol were acetaldehyde and acetone,

dx.doi.org/10.1021/cs5006822 | ACS Catal. 2014, 4, 3463−3469

indicating that the respective subsequent reactions of acetaldehyde and acetone would be slow. Thus, the reaction rates of these compounds were compared. The amounts of unreacted ethanol at GHSV 3×10^5 h^{-1} was 18% (Figure 3a) and that of unreacted acetaldehyde at the same conditions was 59% (Figure 3b). In contrast, that of unreacted acetone at GHSV 1×10^5 h^{-1} was 69% (Figure 9b), although the GHSV value applied was one-third of those for ethanol and acetaldehyde, indicating the low reactivity of acetone. It follows that the slowest step of the current reaction on Sc/In_2O_3 would be the hydrogenation of acetone to form 2-propanol.

Correlation of Property of Surface Acetate Species with the Ketonization Reaction. Surface acetate species, which are the key intermediate for the production of acetone, have been observed on various oxide catalysts. The product yields resulting from the ketonization reaction are dependent on the oxides. Therefore, the correlation of properties of the surface acetate species with the ketonization activity was investigated, and the results revealed the following interesting relationship. At first, the angle of the O−C−O bond in the acetate species produced by the adsorption of acetic acid on the current $Sc3/In_2O_3$ catalyst was compared to that observed during the ethanol adsorption (Figure 7). The bond angles, which were calculated by eq 14[25] using the peak areas of the 1568 and 1444 cm^{-1} IR bands (abbreviated A_{asym} and A_{sym}), were 87.0 and 88.8 deg, respectively. The good agreement between these values indicated that the acetate species produced in the reaction of ethanol adsorbed on the same active site with the same configuration as that of the acetate species originating from the acetic acid adsorption. The results indicated that the values measured upon adsorption of acetic acid can be employed as an index of the surface adsorbates in the ethanol reaction.

$$2\theta = 2 \arctan (A_{asym}/A_{sym})^{0.5} \quad (14)$$

The catalytic activity of various oxides for the ketonization of ethanol was examined at 623−823 K in separate experiments without the cofeed of water and hydrogen for comparison under the same conditions. The results are summarized in Supporting Information, Figure S1 as a function of the reaction temperature and the reaction time. It should be noted that the tested oxides possessed neutral or weak basic−weak acidic surface sites because oxides with strong basic sites or strong acidic sites would not be suitable for the complicated catalysis described above. The respective active temperature ranges were dependent on the oxides, and their catalytic activity increased, decreased, or was stable as the reaction time increased. Therefore, the mean catalytic activity after 2.5 h at the reaction temperature, which affords the maximum activity, was employed as the index for the catalysis. The O−C−O bond angles adsorbed on Sc/In_2O_3 and ZnO were measured here, and the values on SnO_2, TiO_2, CeO_2, and MgO were obtained from the literature,[21−24] because the oxide wafers were very difficult to prepare for the current IR experiments. The catalytic activity is plotted as a function of the O−C−O bond angles of adsorbed acetate species in Figure 10 based on Supporting Information, Table S1. The vertical axis is the total amount of acetone and propene produced based on the assumption that the reaction mechanism was the same as the one on the oxide catalysts examined here. Surprisingly, a typical volcano-shaped dependence was observed. The best O−C−O angle for the ketonization reaction was approximately 90 deg, which was considerably smaller than the angle of free acetic acid, which is 126 degrees. This angle might be related to a $M_2O(CH_3COO)_4$ (M: an active metal ion) intermediate,[26] which may be present on the oxide surfaces for the ketonization of acetic acid. The detailed study of the volcano-shaped dependence is currently under way.

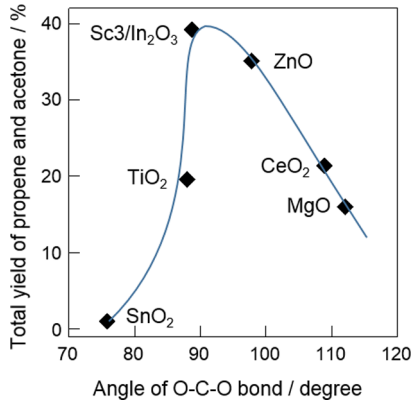

Figure 10. Dependence of catalytic activity on the bond angle of acetate species for the production of acetone and propene.

CONCLUSIONS

The reaction mechanism for the conversion of ethanol to propene on Sc/In_2O_3 was studied using a pulse reaction technique. Acetaldehyde was produced via dehydrogenation of ethanol and directly converted to acetic acid with surface hydroxyl groups, the latter of which was newly confirmed in the current study. Acetic acid was transformed to acetone and carbon dioxide via ketonization. The acetone was reduced to propene with hydrogen via 2-propanol or converted to isobutene without hydrogen. The hydrogenation of acetone to 2-propanol was the slowest step among the consecutive reactions on the Sc/In_2O_3 catalyst. The great difference among the reaction pathways over Ni-M41, Y/CeO_2, and Sc/In_2O_3 may be due to ability of the catalysts to activate the water and hydrogen molecules. It should be noted that the direct conversion of acetaldehyde to acetic acid on Sc/In_2O_3 did not produce ethene as byproduct and resulted in better selectivity to propene than that over Y/CeO_2, because ethyl acetate produced from acetaldehyde on the latter catalyst was an intermediate to yield ethene and acetic acid. In addition, the bond angle of the acetate species adsorbed on the catalyst surface was suggested to be an important factor to determine the reactivity for the ketonization.

ASSOCIATED CONTENT

Supporting Information

The ethanol conversions over six oxide catalysts and the results of IR measurements are summarized in Table S1 and Figure S1. This material is available free of charge via the Internet at http://pubs.acs.org.

AUTHOR INFORMATION

Corresponding Author

*E-mail: iwamotom@tamacc.chuo-u.ac.jp. Tel.: +81-3-3817-1612.

Notes

The authors declare no competing financial interest.

dx.doi.org/10.1021/cs5006822 | ACS Catal. 2014, 4, 3463−3469

■ ACKNOWLEDGMENTS

We wish to acknowledge Grants-in-Aid from the Advanced Low Carbon Technology Program (JST), the Japan Society for the Promotion of Science (JSPS), and the New Energy and Industrial Technology Development Organization (NEDO) of Japan. The authors wish to thank Dr. Tetsuo Suzuki and Mrs. Osamu Takahashi, Hiroshi Ohashi, and Takahiro Kakinuma of the NEDO research group for helpful discussions.

■ REFERENCES

(1) Morschbaker, A. *Polym. Rev.* **2009**, *49*, 79−84.
(2) For example, Olah, G. A.; Molnar, A. *Hydrocarbon Chemistry*, 2nd ed.; John Wiley & Sons, Inc.: Hoboken, NJ, 2003; pp 30−84.
(3) (a) Phillips, C. B.; Datta, R. *Ind. Eng. Chem. Res.* **1997**, *36*, 4466−4475. (b) Brandao, P.; Philippou, A.; Rocha, J.; Anderson, M. W. *Catal. Lett.* **2002**, *80*, 99−102. (c) Aguayo, T.; Gayubo, A. G.; Atutxa, A.; Olazar, M.; Bilbao, J. *Ind. Eng. Chem. Res.* **2002**, *41*, 4216−4224; *J. Chem. Technol. Biotechnol.* **2002**, *77*, 211−216. (d) Gayubo, A. G.; Alonso, A.; Valle, B.; Aguayo, A. T.; Bilbao, J. *Ind. Eng. Chem. Res.* **2010**, *49*, 10836−10844. (e) Gayubo, A. G.; Alonso, A.; Valle, B.; Aguayo, A. T.; Olazar, M.; Bilbao, J. *Chem. Eng. J.* **2011**, *167*, 262−277.
(4) (a) Takahara, I.; Saito, M.; Inaba, M.; Murata, K. *Catal. Lett.* **2005**, *105*, 249−252; **2007**, *113*, 82−85. (b) Inaba, M.; Murata, K.; Saito, M.; Takahara, I. *Green Chem.* **2007**, *9*, 638−646. (c) Song, Z.; Takahashi, A.; Mimura, N.; Fujitani, T. *Catal. Lett.* **2009**, *131*, 364−369. (d) Song, Z.; Takahashi, A.; Nakamura, I.; Fujitani, T. *Appl. Catal., A* **2010**, *384*, 201−205.
(5) (a) Arias, D.; Colmenares, A.; Cubeiro, M. L.; Goldwasser, J.; Lopez, C. M.; Machado, F. J.; Sazo, V. *Catal. Lett.* **1997**, *45*, 51−58. (b) Oikawa, H.; Shibata, Y.; Baba, T. *Appl. Catal., A* **2006**, *312*, 181−185.
(6) (a) Golay, S.; Doepper, R.; Renken, A. *Chem. Eng. Sci.* **1999**, *5*, 4469−4474. (b) Bakoyannakis, D. N.; Zamboulis, D.; Stalidis, G. A.; Deliyanni, E. A. *J. Chem. Technol. Biotechnol.* **2001**, *76*, 1159−1164. (c) Doheim, M. M.; El-Shobaky, H. G. *Coll. Surf. A* **2002**, *204*, 169−174. (d) Zaki, T. *J. Colloid Interface Sci.* **2005**, *284*, 606−613. (e) Varisli, D.; Dogu, T.; Dogu, G. *Chem. Eng. Sci.* **2007**, *62*, 5349−5352; *Ind. Eng. Chem. Res.* **2008**, *47*, 4071−4076; *Ind. Eng. Chem. Res.* **2009**, *48*, 9394−9401. (f) Carrasco-Marin, F.; Mueden, A.; Moreno-Castilla, C. *J. Phys. Chem. B* **1998**, *102*, 9239−9244. (g) Kamiguchi, S.; Chihara, T. *Catal. Lett.* **2003**, *85*, 97−100. (h) Kamiguchi, S.; Nagashima, S.; Komori, K.; Kodomari, M.; Chihara, T. *J. Cluster Sci.* **2007**, *18*, 414−430.
(7) (a) Kamimura, Y.; Sato, S.; Takahashi, R.; Sodesawa, T.; Akashi, T. *Appl. Catal., A* **2003**, *252*, 2399−2407. (b) Nagashima, O.; Sato, S.; Takahashi, R.; Sodesawa, T. *J. Mol. Catal. A* **2005**, *227*, 231−239. (c) Tsuchida, T.; Kubo, J.; Yoshioka, T.; Sakuma, S.; Takeguchi, T.; Ueda, W. *J. Catal.* **2008**, *259*, 183−189.
(8) (a) Kasai, K.; Haishi, T.; Iwamoto, M. *Shokubai* **2007**, *49*, 126−128. (b) Iwamoto, M.; Kasai, K. Japanese Patent No. P2008−255104A.
(9) Iwamoto, M.; Kasai, K.; Haishi, T. *ChemSusChem* **2011**, *4*, 1055−1058.
(10) Sugiyama, S.; Kato, Y.; Wada, T.; Ogawa, S.; Nakagawa, K.; Sotowa, K. *Top. Catal.* **2010**, *53*, 550−554.
(11) (a) Hayashi, F.; Iwamoto, M. *ACS Catal.* **2013**, *3*, 14−17. (b) Hayashi, F.; Tanaka, M.; Lin, M.; Iwamoto, M. *J. Catal.* **2014**, *316*, 112−120.
(12) (a) Mizuno, S.; Kurosawa, M.; Tanaka, M.; Iwamoto, M. *Chem. Lett.* **2012**, *41*, 892−894. (b) Iwamoto, M.; Mizuno, S.; Tanaka, M. *Chem.—Eur. J.* **2013**, *19*, 7214−7220.
(13) (a) Iwamoto, M.; Kosugi, Y. *J. Phys. Chem. C* **2007**, *111*, 13−15. (b) Ikeda, K.; Kawamura, Y.; Yamamoto, T.; Iwamoto, M. *Catal. Commun.* **2008**, *9*, 106−110. (c) Haishi, T.; Kasai, K.; Iwamoto, M. *Chem. Lett.* **2011**, *40*, 624−626.
(14) Klomp, D.; Mashmeyer, T.; Hanefeld, U.; Peters, J. A. *Chem.—Eur. J.* **2004**, *10*, 2088−2093.
(15) (a) Nakajima, T.; Yamaguchi, T.; Tanabe, K. *J. Chem. Soc. Chem. Commun.* **1987**, 394−395. (b) Nakajima, T.; Tanabe, K.; Yamaguchi, T.; Matsuzaki, I.; Mishima, S. *Appl. Catal.* **1989**, *52*, 237−238. (c) Sreerama-Murthy, R.; Patnaik, P.; Sidheswaran, P.; Jayamani, M. *J. Catal.* **1988**, *109*, 298−302. (d) Kamimura, Y.; Sato, S.; Takahashi, R.; Sodesawa, T.; Akashi, T. *Appl. Catal., A* **2003**, *252*, 399−410. (e) Kamimura, Y.; Sato, S.; Takahashi, R.; Sodesawa, T.; Fukui, M. *Chem. Lett.* **2000**, 232−233. (f) Tsuchida, T.; Kubo, J.; Yoshioka, T.; Sakuma, S.; Takeguchi, T.; Ueda, W. *J. Catal.* **2008**, *259*, 183−189.
(16) Sun, J.; Zhu, K.; Gao, F.; Wang, C.; Liu, J.; Peden, C. H. F.; Wang, Y. *J. Am. Soc. Chem.* **2011**, *133*, 11096−11099.
(17) Renz, M. *Eur. J. Org. Chem.* **2005**, 979−988.
(18) Bi, J.; Liu, M.; Song, C.; Wang, X.; Guo, X. *Appl. Catal., B* **2011**, *107*, 68−76.
(19) Sheng, P.-Y.; Bowmaker, G. A.; Idriss, H. *Appl. Catal., A* **2004**, *261*, 171−181.
(20) Idriss, H.; Diagne, C.; Hindermann, J. P.; Kiennemann, A.; Barteau, M. A. *J. Catal.* **1995**, *155*, 219−237.
(21) Pei, Z.-F.; Ponec, V. *Appl. Surf. Sci.* **1996**, *103*, 171−182.
(22) Hasan, M. A.; Zaki, M. I.; Pasupulety, L. *J. Phys. Chem. B* **2002**, *106*, 12747−12756.
(23) Yee, A.; Morrison, S. J.; Idriss, H. *J. Catal.* **1999**, *186*, 279−295.
(24) Kukulska-Zając, E.; Góra-Marek, K.; Datka, J. *Microporous Mesoporous Mater.* **2006**, *96*, 216−221.
(25) Delgass, W. N.; Haller, G. L.; Kellerman, R.; Lunsford, J. H. *Spectroscopy in Heterogeneous Catalysis*; Academic Press: New York, 1979; pp 19−57.
(26) Yamada, Y.; Segawa, M.; Sato, F.; Kojima, T.; Sato, S. *J. Mol. Catal. A* **2011**, *346*, 79−86.